Seventh International Conference on Computational Fluid Dynamics (ICCFD7), Big Island, Hawaii, July 9-13, 2012 **ICCFD7-3201**

Numerical Modelling of Flow in Lower Urinary Tract Using High-Resolution Methods

M. Brandner*, J. Egermaier*, H. Kopincová and J. Rosenberg*

* The University of West Bohemia, Czech republic.

Abstract: The complex model of the lower part of the urinary tract is introduced. It consists of the detrusor smooth muscle cell model and the detailed 1D model of the urethra flow. The nerve control is taken into account. In future this model will allow to simulate the influence of different drugs and mechanical obstructions in the bladder neck and urethra. The urethra flow is solved by a new numerical scheme based on the finite volumes for solving hyperbolic balance laws. Our approach is based on the Riemann solver designed for the augmented quasilinear homogeneous formulation. The scheme has general semidiscrete wave–propagation form and can be extended to arbitrary high order accuracy. It is also well balanced.

Keywords: Urethra flow, well balance, steady states, high-resolution scheme.

1 Introduction

The voiding is a very complex process. As we can see from Fig. 1 it consists of the transfer of information about the state of the bladder filling in to the spinal cord. Next part is the sending of the action potentials to the smooth muscle cells of the bladder. Even this process is not simple and includes the spreading of the action potential along the nerve axon and the transmission of the mediator (Ach - acetylcholine) in the synapse. The action potential starts the process of the smooth muscle contraction.

The smooth muscles have a lot of different forms in contradiction with the striated muscles. They are present in vesicles, arteries and others hollow organs.

Although the own biological motor - sliding between actin and myosin fueled by hydrolysis of ATP- is the same here as well as in striated and heart muscles, there are important differences between these basic types of muscles and also between smooth muscles in different organs. The sliding between actin and myosin causing the change of the form (length) of the muscle cell and its stiffness can be observed as a kind of growth and remodeling. This approach described e.g. in [1] and [2] is used in this model. It should be mentioned that a lot of different smooth muscle cells (SMC) models exist. They are based either on Huxley model where the calcium dynamics is not taken into account in details or on the contrary the calcium dynamics and the phosphorylation is modeled very precisely but the mechanochemical coupling is based on the work on [3] where the stress in the muscle cell depends linearly on the amount of the bonded cross-bridges either phosphorylated or unphosphorylated (e.g. [4], [5], where the model is applied to the SMC in the vessels).

To be able to describe the very complex processes in the SMC in the efficient form it is necessary to use the irreversible thermodynamics. This approach was described in [6].

Using all these approaches the algorithm published in [7] was developed. In this contribution we join on the results of this paper. The simple model of the whole bladder and the detailed 1D model of the urethra flow is added. Some examples of the numerical experiments are shown.

2 Bladder contraction

As it was already mentioned, the whole model of the bladder contraction is described in [8]. It consists of the following parts:

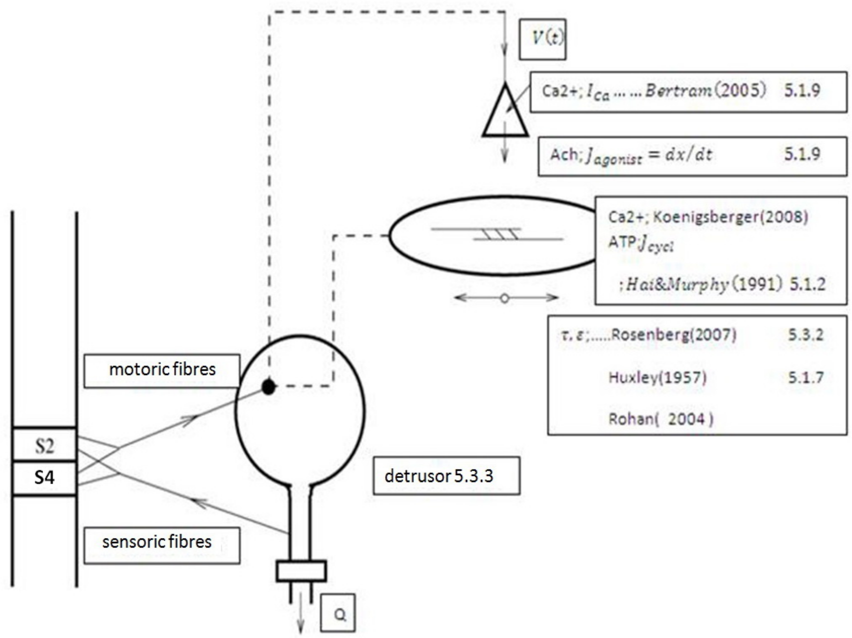

Figure 1:

- Model of the time evolution of the Ca^{2+} concentration - five equations. The Ca^{2+} intracellular concentration is the main control parameter for the next processes and finally for the smooth muscle contraction. Its increase depends on the flux $J_{agonist}$ of the mediator (in this case acetylcholine) via the nerve synapse.

$$
\begin{aligned}
\frac{dc}{dt} &= J_{IP3} - J_{VOCC} + J_{Na/Ca} - J_{SRuptake} + J_{CICR} - J_{extrusion} + J_{leak} + 0.1 J_{stretch} \\
\frac{ds}{dt} &= J_{SRuptake} - J_{CICR} - J_{leak} \\
\frac{dv}{dt} &= \gamma(-J_{Na/K} - J_{Cl} - 2J_{VOCC} - J_{Na/Ca} - J_K - J_{stretch}) \\
\frac{dw}{dt} &= \lambda K_{activate} \\
\frac{dI}{dt} &= J_{agonist} - J_{degrad}
\end{aligned} \tag{1}
$$

  where the unknown functions represents the following: $c = c(t)$ calcium concentration in cytoplasm, $s = s(t)$ calcium concentration in ER/SR, $v = v(t)$ membrane tension, $w = w(t)$ probability of opening channels activated by Ca^{2+} and $I = I(t)$ IP3 sensitive reservoirs concentration in cytoplasm. For details and complete description of the functions and parameters see [5]

- Model of the time evolution of the phosphorylation of the light myosin chain - three equations. The muscle cell contraction is caused by the relative movement of the myosin and actin filaments. For this it is necessary that the phosphorylation of the mentioned light myosin chain on the heads of the myosin occurs.

$$\begin{aligned}
\frac{dA_M}{dt} &= k_5 A_{M_p} - (k_7 + k_6) A_M, \\
\frac{dA_{M_p}}{dt} &= k_3 M_p + k_6 A_M - (k_4 + k_5) A_{M_p}, \\
\frac{dM_p}{dt} &= k_1(1 - A_M) + (k_4 - k_1) A_{M_p} - (k_1 + k_2 + k_3) M_p,
\end{aligned} \tag{2}$$

where the unknown functions represent the following: $A_M = A_M(t)$ connected cross-bridges, $A_{M_p} = A_{M_p}(t)$ connected phosphorylated cross-bridges and $M_p = M_p(t)$ unconnected phosphorylated cross-bridges. $k_6 = k_6(c)$, the other terms k_i are constant. For details and complete description of the functions and parameters see [3]. Knowing this process also the time evolution of the ATP consumption (J_{cycl}) can be determined. The ATP (adenosintriphosphate) is the main energy source for the muscle contraction.

$$\frac{dY}{dt} = -Q_Q Y + L J_{cycl}, \tag{3}$$

where $Y = Y(t)$ represents the ATP concentration, Q_Q is the damping parameter and L is the constant.

3 Model of the own contraction based on the GRT and the irreversible thermodynamics

The growth and remodelling theory [9] together with the laws of irreversible thermodynamics with internal variables was applied in [6] to describe the mechano-chemical coupling of the smooth muscle cell contraction. The product of the chemical reaction affinity (the ATP hydrolysis) with its rate plays an important role in the discussed model. Further it can be assumed that the rate of the ATP hydrolysis depends on the ATP consumption. The corresponding equations in the non-dimensional form are following:

$$\begin{aligned}
\dot{x} &= k_1 \left[\tau - z(x-1)\right], \\
\dot{y} &= \frac{y}{k_2}\left[x\tau - \frac{1}{2}z(x-1)^2 + C'\right], \qquad (4)\\
\dot{z} &= \mathrm{sgn}(m) \cdot \left[r - \frac{1}{2}z(x-1)^2\right], \qquad (5)
\end{aligned}$$

where

$$x = \frac{l}{l_r}, y = \frac{l_r}{l_0},$$

l_0 is the initial length of the muscle fibre, l_r its length after stimulation when the fibre is unloaded (s. c. resting length), l the actual length (when the contraction is isometric this is the input value), τ the stress and k is the fibre stiffness, m and r are constants. The non-dimensional values are labeled with the single quote mark. The others symbols are the parameters. The most important parameter is C'. Using the irreversible thermodynamics we can obtain the following relations

$$\begin{aligned}
C' &= p_c \cdot (C - a_{chem} Y)\sqrt{\frac{|m|}{g}}, \\
C\sqrt{\frac{|m|}{g}} &= C_0 + C_t e^{q_c\left(\frac{l}{l_0} - \frac{l}{l_0}|_{opt}\right)^2}, \\
p_c &= p_{c_0} e^{s_c\left(\frac{l}{l_0} - \frac{l}{l_0}|_{opt}\right)^2},
\end{aligned} \tag{6}$$

where for the afinity of the chemical reactions especially for the hydrolysis of the ATP

$$a_{chem} = -Q \cdot Y. \tag{7}$$

Y is the concentration of ATP determined by equation (3) and $C_0, C_t, a_{chem}, q_c, s_c, g, p_{c_0}, Q$ are constant parameters. Than the whole model is finished because the ATP consumption J_{cycl} as a function of the Ca^{2+} concentration in the cytoplasm was already determined.

4 Bladder and voiding model

To model the contraction of the bladder during the voiding process we will use the very simple model according [11] and [12]. The bladder is modelled as a hollow sphere with the output corresponding to the input into urethra.

For the pressure in the bladder the following formula is introduced in [11]

$$p = \frac{V_{sh}}{3V} \cdot \tau, \qquad \tau = \frac{F}{S}, \tag{8}$$

where V_{sh} is the volume of the wall, V the inner volume, τ stress in the muscle fibre, S the inner surface and F the force in the muscle cell.

For the flux q we have

$$q = \frac{dV}{dt}, \tag{9}$$

where ρ is the density of the fluid.

Using the formulas for the isotonic contraction, we can at first obtain the relation for the volume. The following holds

$$l' = \frac{l}{l_0} = x \cdot y \tag{10}$$

and then

$$V = \kappa \cdot (x \cdot y)^3, \tag{11}$$

where κ is the constant which in the theoretical case if only one cell will occupy the circumference of the spherical bladder will be $1/6\pi^2$. Putting this formula into the equation for q and using the equations for the derivatives of x and y mentioned before we obtain the equation, from which we can calculate τ:

$$\tau = \frac{\frac{-q}{3\kappa(x \cdot y)^2} + \left[k_1 z y (x-1) + \frac{zyx}{2k_2}(x-1)^2 - \frac{xy}{k_2} C'\right]}{k_1 y + \frac{x^2 y}{k_2}}. \tag{12}$$

For the pressure, the following equality holds

$$p = \frac{V_{sh}}{3\kappa \cdot (x \cdot y)^3} \cdot \frac{\frac{-q}{3\kappa(x \cdot y)^2} + \left[k_1 z y (x-1) + \frac{zyx}{2k_2}(x-1)^2 - \frac{xy}{k_2} C'\right]}{k_1 y + \frac{x^2 y}{k_2}}. \tag{13}$$

This will be putted into the equations for the isotonic contraction.

5 Urethra flow

We now briefly introduce a problem describing fluid flow through the elastic tube represented by hyperbolic partial differential equations with the source term. In the case of the male urethra, the system based on model in [13] has the following form

$$\begin{aligned} a_t + q_x &= 0, \\ q_t + \left(\frac{q^2}{a} + \frac{a^2}{2\rho\beta}\right)_x &= \frac{a}{\rho}\left(\frac{a_0}{\beta}\right)_x + \frac{a^2}{2\rho\beta^2}\beta_x - \frac{q^2}{4a^2}\sqrt{\frac{\pi}{a}}\lambda(Re), \end{aligned} \tag{14}$$

where $a = a(x,t)$ is the unknown cross-section area, $q = q(x,t)$ is the unknown flow rate (we also denote $v = v(x,t)$ as the fluid velocity, $v = \frac{q}{a}$), ρ is the fluid density, $a_0 = a_0(x)$ is the cross-section of the tube under no pressure, $\beta = \beta(x,t)$ is the coefficient describing tube compliance and $\lambda(Re)$ is the Mooney-Darcy friction factor ($\lambda(Re) = 64/Re$ for laminar flow). Re is the Reynolds number defined by

$$Re = \frac{\rho q}{\mu a}\sqrt{\frac{4a}{\pi}}, \tag{15}$$

where μ is fluid viscosity. This model contains constitutive relation between the pressure and the cross section of the tube

$$p = \frac{a - a_0}{\beta} + p_e, \tag{16}$$

where p_e is surrounding pressure.

Presented system (14) can be written in the compact matrix form

$$\mathbf{u}_t + [\mathbf{f}(\mathbf{u},x)]_x = \boldsymbol{\psi}(\mathbf{u},x), \tag{17}$$

with $\mathbf{q}(x,t)$ being the vector of conserved quantities, $\mathbf{f}(\mathbf{q},x)$ the flux function and $\boldsymbol{\psi}(\mathbf{q},x)$ the source term. This relation represents the balance laws. For the following consideration, we reformulate this problem to the nonconservative form.

5.1 Nonconservative problems

We consider the nonlinear hyperbolic problem in nonconservative form

$$\begin{aligned} \mathbf{u}_t + \mathbf{A}(\mathbf{u})\mathbf{u}_x &= \mathbf{0},\ x \in \mathbf{R},\ t \in (0,T), \\ \mathbf{u}(x,0) &= \mathbf{u}_0(x),\ x \in \mathbf{R}, \end{aligned} \tag{18}$$

The numerical schemes for solving problems (18) can be written in fluctuation form

$$\frac{\partial \mathbf{U_j}}{\partial t} = -\frac{1}{\Delta x}[\mathbf{A}^-(\mathbf{U}^-_{j+1/2}, \mathbf{U}^+_{j+1/2}) + \mathbf{A}(\mathbf{U}^-_{j+1/2}, \mathbf{U}^+_{j-1/2}) + \mathbf{A}^+(\mathbf{U}^-_{j-1/2}, \mathbf{U}^+_{j-1/2})], \tag{19}$$

where $\mathbf{A}^\pm(\mathbf{U}^-_{j+1/2}, \mathbf{U}^+_{j+1/2})$ are so called fluctuations. They can be defined by the sum of waves moving to the right or to the left. The directions are dependent on the signs of the speeds of these waves, which are related to the eigenvalues of matrix $\mathbf{A}(\mathbf{u})$. In what follows, we use the notation $\mathbf{U}^+_{j+1/2}$ and $\mathbf{U}^-_{j+1/2}$ for the reconstructed values of unknown function. Reconstructed values represent the approximations of limit values at the points $x_{j+1/2}$. The most common reconstructions are based on the minmod function (see for example [14]) or ENO and WENO techniques [15].

The reconstruction can be applied to each component of $\mathbf{u}$. But this approach does not work well in general. It is better to apply the reconstruction to the characteristic field of $\mathbf{u}$. It means that each jump is decomposed to the eigenvectors $\mathbf{r}$ of Jacobian matrix $\mathbf{A}(\mathbf{u})$.

$$\mathbf{U}_{j+1} - \mathbf{U}_j = \sum_{p=1}^{m} \alpha^p_{j+1/2}\mathbf{r}^p_{j+1/2}. \tag{20}$$

Then the reconstruction based on minmod function can be defined by following

$$\begin{aligned} \mathbf{U}^+_{j+1/2} &= \mathbf{U}_{j+1} + \sum_p \phi^{p,+}_{I+1/2}\alpha^p_{j+1/2}\mathbf{r}^p_{j+1/2}, \\ \mathbf{U}^-_{j+1/2} &= \mathbf{U}_j + \sum_p \phi^{p,-}_{I+1/2}\alpha^p_{j+1/2}\mathbf{r}^p_{j+1/2}, \end{aligned} \tag{21}$$

where

$$\phi^{p,\pm}_{I+1/2} = \mp\frac{1}{2}\left(1 + \mathrm{sgn}(\theta^p_{I+1/2})\right)\min(1, |\theta^p_{I+1/2}|) \tag{22}$$

and

$$I = \begin{cases} j-1/2, & \text{if } s^p_{j+1/2} \geq 0, \\ j+3/2, & \text{if } s^p_{j+1/2} < 0. \end{cases} \tag{23}$$

The function $\theta^p_{j+1/2}$ can be determined by the following way

$$\theta^p_{j+1/2} = \frac{\alpha^p_{j+1/2}\mathbf{r}^p_{j+1/2} \cdot \mathbf{r}^p_{I+1/2}}{\alpha^p_{I+1/2}\mathbf{r}^p_{I+1/2} \cdot \mathbf{r}^p_{I+1/2}}. \tag{24}$$

When the problem (18) is derived from the conservation form (17), i.e. $\mathbf{f}'(\mathbf{u}) = \mathbf{A}(\mathbf{u})$ is the Jacobi matrix of the system, fluctuations can be defined as follows

$$\begin{array}{rcl} \mathbf{A}(\mathbf{U}^-_{j+1/2}, \mathbf{U}^+_{j-1/2}) & = & \mathbf{f}(\mathbf{U}^-_{j+1/2}) - \mathbf{f}(\mathbf{U}^+_{j-1/2}), \\ \mathbf{A}^-(\mathbf{U}^-_{j+1/2}, \mathbf{U}^+_{j+1/2}) & = & \mathbf{F}^-_{j+1/2} - \mathbf{f}(\mathbf{U}^-_{j+1/2}), \\ \mathbf{A}^+(\mathbf{U}^-_{j-1/2}, \mathbf{U}^+_{j-1/2}) & = & \mathbf{f}(\mathbf{U}^+_{j-1/2}) - \mathbf{F}^+_{j-1/2}. \end{array} \tag{25}$$

5.2 Decompositions based on augmented system

This procedure is based on the extension of the system (14) by other equations (for simplicity we omit viscous term). This was derived in [16] for the shallow water flow. The advantage of this step is in the conversion of the nonhomogeneous system to the homogeneous one. In the case of urethra flow we obtain the system of four equations, where the augmented vector of unknown functions is $\mathbf{w} = [a, q, \frac{a_0}{\beta}, \beta]^T$. Furthermore we formally augment this system by adding components of the flux function $\mathbf{f}(\mathbf{u})$ to the vector of the unknown functions. We multiply balance law (17) by Jacobian matrix $\mathbf{f}'(\mathbf{u})$ and obtain following relation

$$\mathbf{f}'(\mathbf{u})\mathbf{u}_t + \mathbf{f}'(\mathbf{u})[\mathbf{f}(\mathbf{u})]_x = \mathbf{f}'(\mathbf{u})\boldsymbol{\psi}(\mathbf{u}, x). \tag{26}$$

Because of $\mathbf{f}'(\mathbf{u})\mathbf{u}_t = [\mathbf{f}(\mathbf{u})]_t$ we obtain hyperbolic system for the flux function

$$[\mathbf{f}(\mathbf{u})]_t + \mathbf{f}'(\mathbf{u})[\mathbf{f}(\mathbf{u})]_x = \mathbf{f}'(\mathbf{u})\boldsymbol{\psi}(\mathbf{u}, x). \tag{27}$$

In the case of the urethra fluid flow modelling we add only one equation for the second component of the flux function i.e. $\phi = av^2 + \frac{a^2}{2\rho\beta}$ (the first component q is unknown function of the original balance law), which has the form

$$\phi_t + (-v^2 + \frac{a}{2\rho\beta})(av)_x + 2v\phi_x - \frac{2av}{\rho}\left(\frac{a_0}{\beta}\right)_x - \frac{a^2 v}{\rho\beta^2}\beta_x = 0. \tag{28}$$

Finally augmented system can be written in the nonconservative form

$$\begin{bmatrix} a \\ q \\ \phi \\ \frac{a_0}{\beta} \\ \beta \end{bmatrix}_t + \begin{bmatrix} 0 & 1 & 0 & 0 & 0 \\ -\frac{q^2}{a^2} + \frac{a}{\rho\beta} & 2\frac{q}{a} & 0 & -\frac{a}{\rho} & -\frac{a^2}{\rho\beta^2} \\ 0 & -\frac{q^2}{a^2} + \frac{a}{\rho\beta} & 2\frac{q}{a} & 2\frac{q}{\rho} & -\frac{aq}{\rho\beta^2} \\ 0 & 0 & 0 & 0 & 0 \\ 0 & 0 & 0 & 0 & 0 \end{bmatrix} \begin{bmatrix} a \\ q \\ \phi \\ \frac{a_0}{\beta} \\ \beta \end{bmatrix}_x = \mathbf{0}, \tag{29}$$

briefly $\mathbf{w}_t + \mathbf{B}(\mathbf{w})\mathbf{w}_x = \mathbf{0}$, where matrix $\mathbf{B}(\mathbf{w})$ has following eigenvalues

$$\lambda^1 = v - \sqrt{\frac{a}{\rho\beta}}, \lambda^2 = v + \sqrt{\frac{a}{\rho\beta}}, \lambda^3 = 2v, \lambda^4 = \lambda^5 = 0 \tag{30}$$

and corresponding eigenvectors

$$\mathbf{r}^1 = \begin{bmatrix} 1 \\ \lambda^1 \\ (\lambda^1)^2 \\ 0 \\ 0 \end{bmatrix}, \mathbf{r}^2 = \begin{bmatrix} 1 \\ \lambda^2 \\ (\lambda^2)^2 \\ 0 \\ 0 \end{bmatrix}, \mathbf{r}^3 = \begin{bmatrix} 0 \\ 0 \\ 1 \\ 0 \\ 0 \end{bmatrix}, \mathbf{r}^4 = \begin{bmatrix} \frac{-a}{\rho\lambda^1\lambda^2} \\ 0 \\ \frac{a}{\rho} \\ 1 \\ 0 \end{bmatrix}, \mathbf{r}^5 = \begin{bmatrix} \frac{-a^2}{\rho\beta^2\lambda^1\lambda^2} \\ 0 \\ \frac{a^2}{2\rho\beta^2} \\ 0 \\ 1 \end{bmatrix}. \tag{31}$$

We have five linearly independent eigenvectors. The approximation is chosen to be able to prove the consistency and provide the stability of the algorithm. In some special cases this scheme is conservative and we can guarantee the positive semidefiniteness, but only under the additional assumptions (see [17]).

The fluctuations are then defined by

$$\begin{aligned} \mathbf{A}^-(\mathbf{U}^-_{j+1/2}, \mathbf{U}^+_{j+1/2}) &= \begin{bmatrix} 0 & 1 & 0 & 0 & 1 \\ 0 & 1 & 0 & 0 & 1 \end{bmatrix} \cdot \sum_{p=1, s^{p,n}_{j+1/2}<0}^{m} \gamma^p_{j+1/2}\mathbf{r}^p_{j+1/2}, \\ \mathbf{A}^+(\mathbf{U}^-_{j+1/2}, \mathbf{U}^+_{j+1/2}) &= \begin{bmatrix} 0 & 1 & 0 & 0 & 1 \\ 0 & 1 & 0 & 0 & 1 \end{bmatrix} \cdot \sum_{p=1, s^{p,n}_{j+1/2}>0}^{m} \gamma^p_{j+1/2}\mathbf{r}^p_{j+1/2}, \\ \mathbf{A}(\mathbf{U}^+_{j-1/2}, \mathbf{U}^-_{j+1/2}) &= \mathbf{f}(\mathbf{U}^-_{j+1/2}) - \mathbf{f}(\mathbf{U}^+_{j-1/2}) - \mathbf{\Psi}(\mathbf{U}^-_{j+1/2}, \mathbf{U}^+_{j-1/2}), \end{aligned} \tag{32}$$

where $\mathbf{\Psi}(\mathbf{U}^-_{j+1/2}, \mathbf{U}^+_{j-1/2})$ is a suitable approximation of the source term and $\mathbf{r}^p_{j+1/2}$ are suitable approximations of the eigenvectors (31).

5.3 Steady states

It is very important to choose such approximation which conserves steady states, if these states occur exactly. Steady states mean that $\mathbf{u}_t = \mathbf{0}$ and therefore $[\mathbf{f}(\mathbf{u})]_x = \boldsymbol{\psi}(\mathbf{u}, x)$. The steady state in the urethra modeling means

$$\begin{aligned} q_x &= 0, \\ \left(\frac{q^2}{a} + \frac{a^2}{2\rho\beta}\right)_x &= \frac{a}{\rho}\left(\frac{a_0}{\beta}\right)_x + \frac{a^2}{2\rho\beta^2}\beta_x. \end{aligned} \tag{33}$$

The first equation implies that $q = av$ is always constant for steady states. We consider that the parameters β and $\frac{a_0}{\beta}$ are smooth and vary monotonically only in small neighborhoods $(x_j - \epsilon_j, x_j + \epsilon_j)$ of the point x_j so that β_x and $\left(\frac{a_0}{\beta}\right)_x$ do not change sign in this interval and are zero out of this interval. The second equation can be rewritten as

$$\left(-v^2 + \frac{a}{\rho\beta}\right)a_x = \frac{a}{\rho}\left(\frac{a_0}{\beta}\right)_x + \frac{a^2}{\rho\beta^2}\beta_x. \tag{34}$$

It can be seen that (34) is equivalent to

$$\left(\frac{v^2}{2} + \frac{a - a_0}{\rho\beta}\right)_x = 0. \tag{35}$$

This means that the term $\frac{v^2}{2} + \frac{a-a_0}{\rho\beta}$ is constant for differentiable steady states. Therefore the following property must be satisfied

$$\left(\frac{v^2}{2} + \frac{a - a_0}{\rho\beta}\right)_j = \left(\frac{v^2}{2} + \frac{a - a_0}{\rho\beta}\right)_{j+1}. \tag{36}$$

Using (36) we can express the discrete relation analogous to the smooth one $\phi_x = \frac{a}{\rho}\left(\frac{a_0}{\beta}\right)_x + \frac{a^2}{2\rho\beta^2}\beta_x$

$$\Delta\Phi = \frac{\widetilde{\lambda^1\lambda^2}}{\overline{\lambda^1\lambda^2}}\frac{\bar{A}}{\rho}\Delta\left(\frac{a_0}{\beta}\right) + \left(\frac{\widetilde{\lambda^1\lambda^2}}{\overline{\lambda^1\lambda^2}}\frac{\bar{A}^2}{\rho\beta_{j+1}\beta_j} - \frac{\tilde{A}^2}{2\rho\beta_{j+1}\beta_j}\right)\Delta\beta. \tag{37}$$

where for j-th cell $\Delta(.) = (.)_{j+1} - (.)_j$, $\bar{A} = \frac{A_j + A_{j+1}}{2}$, $\bar{\beta} = \frac{\beta_j+\beta_{j+1}}{2}$, $\tilde{A}^2 = \frac{A_j^2 + A_{j+1}^2}{2}$, $\tilde{V}^2 = |V_j V_{j+1}|$, $\bar{V}^2 = \left(\frac{V_j+V_{j+1}}{2}\right)^2$ and

$$\widetilde{\lambda^1\lambda^2} = -\tilde{V}^2 + \frac{\bar{A}\bar{\beta}}{\rho\beta_{j+1}\beta_j}, \qquad \overline{\lambda^1\lambda^2} = -\bar{V}^2 + \frac{\bar{A}\bar{\beta}}{\rho\beta_{j+1}\beta_j}. \tag{38}$$

The steady state for the augmented system means $\mathbf{B}(\mathbf{w})\mathbf{w}_x = \mathbf{0}$, therefore $\mathbf{w}_x$ is a linear combination of the eigenvectors corresponding to the zero eigenvalues. The discrete form of the vector $\Delta\mathbf{w}$ corresponds to the certain approximation of these eigenvectors. It can be shown that

$$\Delta\begin{bmatrix} A \\ Q \\ \Phi \\ \frac{a_0}{\beta} \\ \beta \end{bmatrix} = \begin{bmatrix} \frac{\bar{A}}{\rho}\frac{1}{\overline{\lambda^1\lambda^2}} \\ 0 \\ \frac{\bar{A}}{\rho}\frac{\widetilde{\lambda^1\lambda^2}}{\overline{\lambda^1\lambda^2}} \\ 1 \\ 0 \end{bmatrix}\Delta\left(\frac{a_0}{\beta}\right) + \begin{bmatrix} \frac{\bar{A}^2}{\rho\beta_{j+1}\beta_j}\frac{1}{\overline{\lambda^1\lambda^2}} \\ 0 \\ \frac{\bar{A}^2}{\rho\beta_{j+1}\beta_j}\frac{\widetilde{\lambda^1\lambda^2}}{\overline{\lambda^1\lambda^2}} - \frac{\tilde{A}^2}{2\rho\beta_{j+1}\beta_j} \\ 0 \\ 1 \end{bmatrix}\Delta\beta. \tag{39}$$

Therefore we use vectors on the RHS of (39) as approximations of the fourth and fifth eigenvectors of the matrix $\mathbf{B}(\mathbf{w})$. Then the fluctuations (32) are defined with these vectors and the approximation of the source term is defined by the third line in (39)

$$\mathbf{\Psi}(\mathbf{U}^-_{j+1/2}, \mathbf{U}^+_{j-1/2}) = \frac{\bar{A}}{\rho}\frac{\widetilde{\lambda^1\lambda^2}}{\overline{\lambda^1\lambda^2}}\Delta\left(\frac{a_0}{\beta}\right) + \frac{\bar{A}^2}{\rho\beta_{j+1}\beta_j}\frac{\widetilde{\lambda^1\lambda^2}}{\overline{\lambda^1\lambda^2}} - \frac{\tilde{A}^2}{2\rho\beta_{j+1}\beta_j}\Delta\beta, \tag{40}$$

where the values $(.)_j$ and $(.)_{j+1}$ should be replaced by their appropriate reconstructed values $(.)^+_{j-1/2}$ and $(.)^-_{j+1/2}$.

5.4 Positive semidefiniteness

Positive semidefiniteness of this scheme is shown in [16] for the case of shallow water equation. It is based on a special choice of approximations of the eigenvectors (31). This, in the case of urethra flow, is more complicated because of the structure of the eigenvectors. Some necessary conditions for approximation of these eigenvectors are presented in [17].

6 Numerical experiment of the urethra flow

The fluid flow is described by the system (14). Initial conditions are chosen by the following values of the intravesical pressure and the velocity of the fluid

$$p(x,0) = \begin{cases} 3000\ \text{Pa}, & \text{if } x = 0 \\ 500\ \text{Pa}, & \text{otherwise,} \end{cases}, v(x,0) = \begin{cases} 1\ \text{m/s}, & \text{if } x = 0 \\ 0\ \text{m/s}, & \text{otherwise,} \end{cases} \tag{41}$$

Boundary conditions in the point $x = 0$ are chosen so that there would be constant flow rate, the fluid velocity is computed by the Riemann invariants (see [18]). On the output of the urethra at the point $x = 0.19$ the velocity and cross section of the urethra are also computed by the Riemann invariants but in certain cases it is necessary to use different technique (see [18] again). The shape of parameter $\beta = \beta(x)$, the initial and steady state is captured on the figure 2. It can be seen that the method preserves general steady state. It is confirmed by the constant flow rate through the hole urethra at the last figure 2. For the comparison see

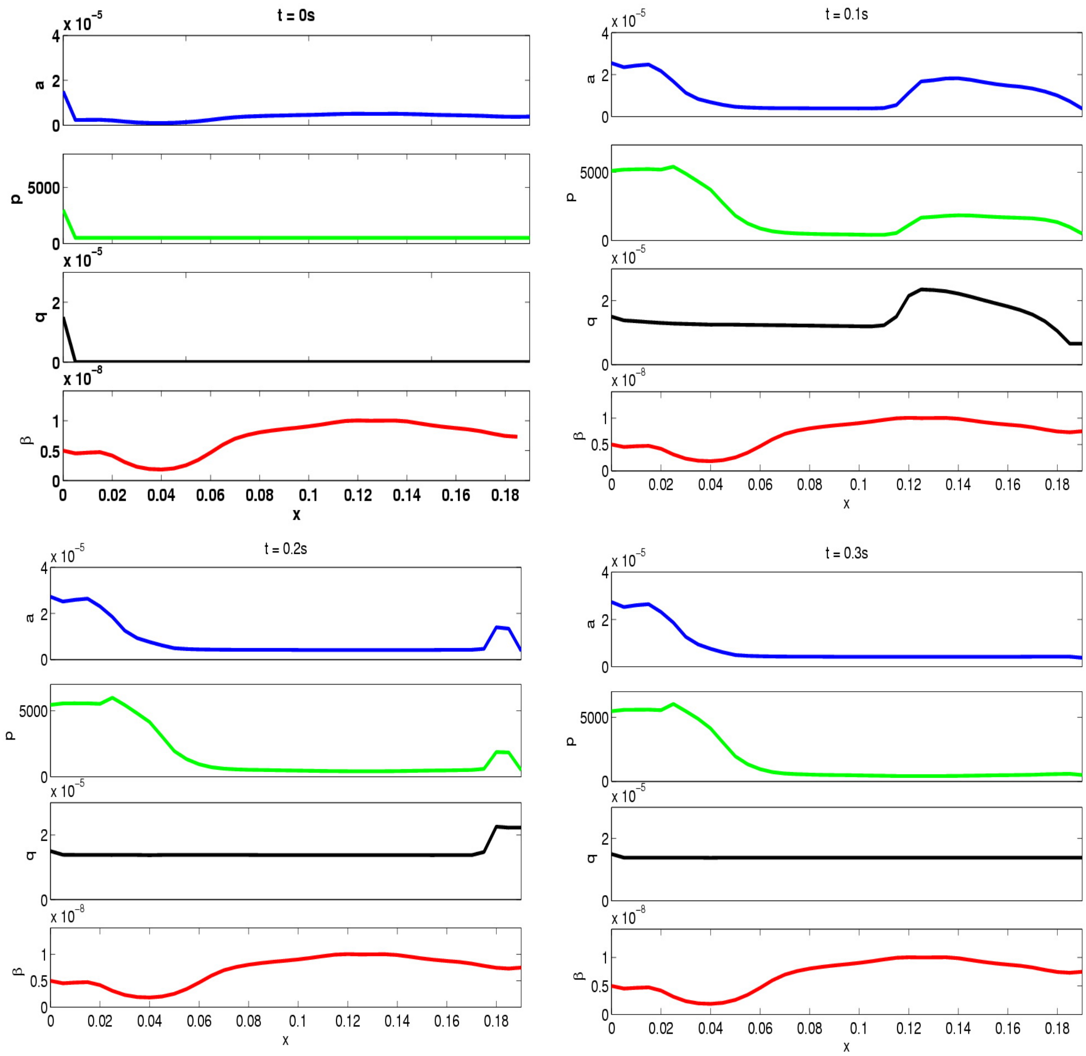

Figure 2: Time evolution of the quantities through the urethra (cross section area, pressure, flow rate, tube compliance) - well balanced scheme.

the figure **??**, where the same experiment computed by the the method which do not preserves steady state is illustrated.

7 Complex model of the bladder and the urethra

The whole voiding model consists of the detrusor smooth muscle cell model and the model of the urethra flow. It is described by the system of following ordinary differential equations:

- 12 equations describing the bladder model and the detrusor contraction during voiding - the systems (1), (2) and (4).
- $2J$ equations of urethra flow, where J is the number of finite volumes which divide the urethra region

The connection between the detrusor model and urethra flow is implemented by by the relations (12), (13) and the constitutive relation (16). The outflow of the bladder is the same as the flow rate in the first finite volume of the urethra region. So the pressure of the bladder is dependent on the flow rate in the tube (13).

The cross-section in the first finite volume of the urethra region is then given by the constitutive relation (16). From the view of urethra flow, the inflow boundary condition consists of the given cross-section and extrapolation of the flow rate from the urethra region.

8 Numerical experiment including the complex model of lower urinary tract

Now we present numerical experiment based on the system of differential equations described detrusor smooth muscle cell model (12 equations) and urethral flow (30 equations). The equations describing urethral flow are based on spatial high-resolution discretization of the urethra (15 finite volumes) described in section 5.2 The parameters used in this experiment are the same as in [8]. The figures 3 illustrate time evolution of the quantities at the bladder neck. For the further application it is necessary to fit the parameters because of non-dimensionality of the equations describing the muscle contraction.

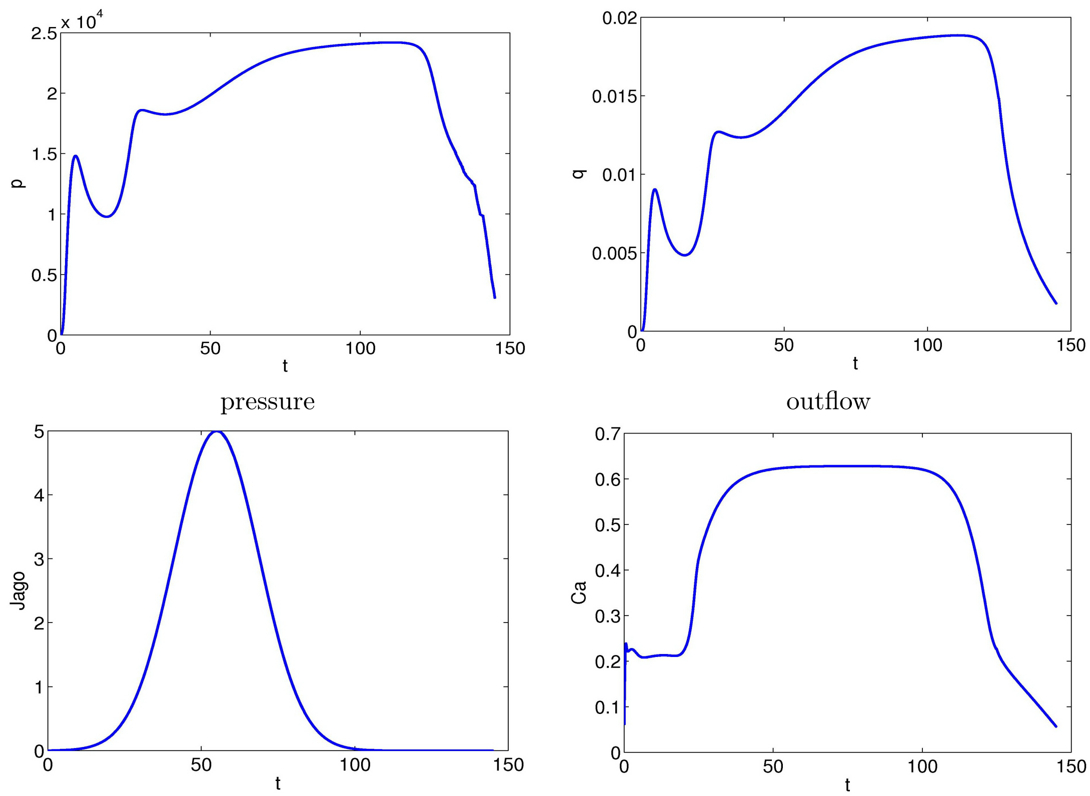

pressure outflow

mediator flux Ca^{2+} concentration

Figure 3: Time evolution of the quantities at the bladder neck.

1. For the simplicity the precious modelling of the synapse is neglected and the mediator flux $J_{agonist}$ is chosen - see Fig. 3. The IC units are used although in the medical paper are used for intravesical pressure cm H_2O (1 cm $H_2O = 0.1$ kPa) and for the outflow ml/s. The concentration is measured in μM where M = mol/l.

2. At the Fig. 4 there are shown the cross-section area, velocity and flow rate along the whole urethra in two different times after beginning of voiding.

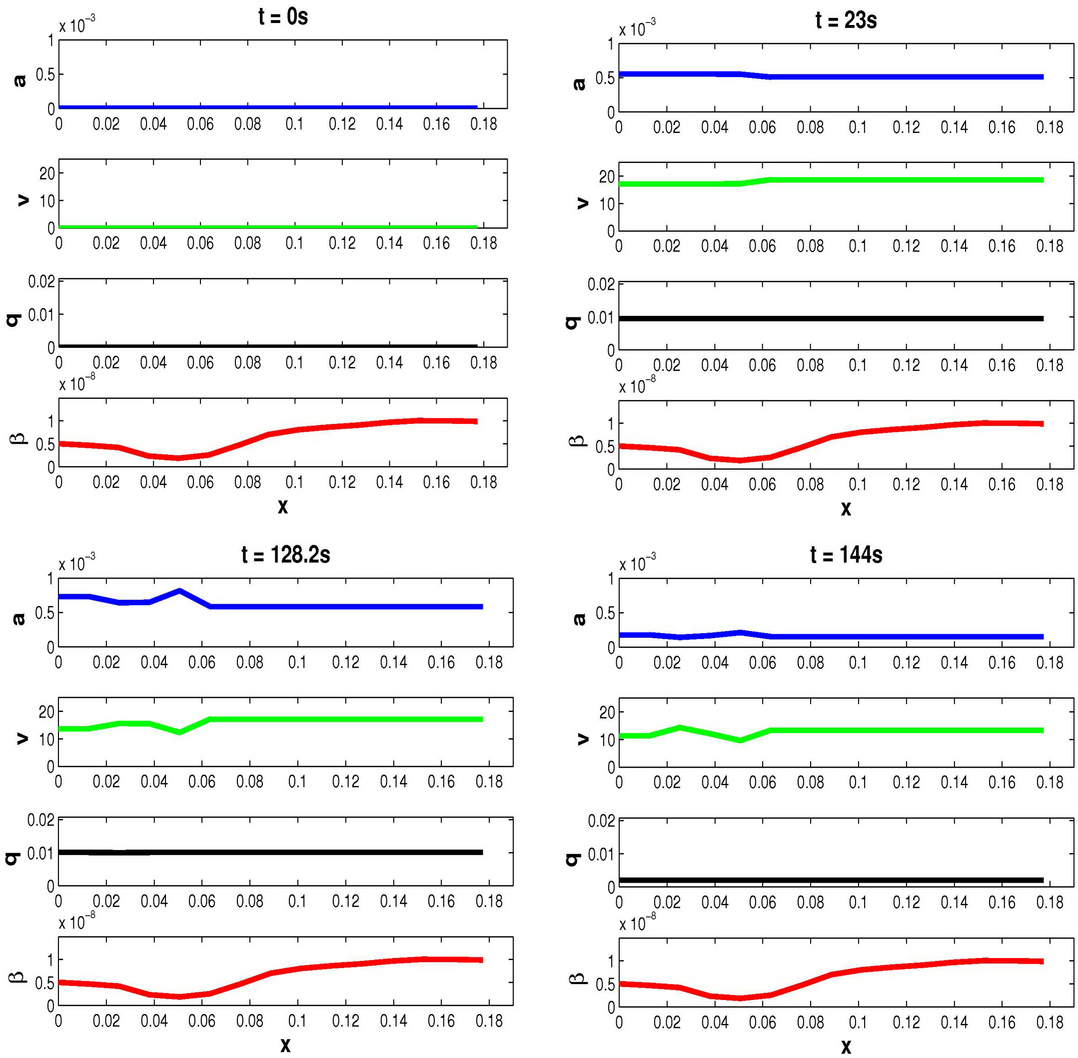

Figure 4: Time evolution of the quantities through the urethra (cross section area, velocity, flow rate, tube compliance).

9 Conclusion

We presented the complex model of the lower part of the urinary tract. A simple bladder model and the detrusor contraction model were developed during voiding together with the detailed model of urethra flow. The urethra flow was described by the high-resolution positive semidefiniteness method, which preserves general steady states. For the practical application the identification of the parameters is necessary.

Acknowledgments

This work was supported by the European Regional Development Fund (ERDF), project NTIS - New Technologies for Information Society, European Centre of Excellence, CZ.1.05/1.1.00/02.0090 and the project SGS-2010-077 Support of Biomechanics at the Faculty of Applied Sciences, University of West Bohemia in Pilsen.

References

[1] J. Rosenberg and L. Hynčík. Modelling of the influance of the stifness evolution on the behaviour of the Muscle fibre. Human Biomechanics, International Conference, 29.9.-1.10.2008 Praha, Czech Republic, 2008.

[2] J. Rosenberg and L. Hynčík. Contribution to the simulation of growth and remodelling applied to Muscle fibre stimulation. Short communication of the 1st IMACS International Conference on Computational Biomechanice and Biology ICCBB, Sept. 10-13, Plzeň, Czech Republic, 2007.

[3] C.M. Hai and R.A. Murphy. Adenosine 5'-triphosphate consumption by smooth muscle as predicted by the coupled four-state crossbridge model. *Biophysical Journal*, 61(2):530–541, 1992.

[4] Edwards D.H. Hill C.E. Griffith T.M. Parthimos, D. Dynamics of a three-variable nonlinear model of vasomotion: Comparison of theory and experiment. *Biophysical Journal*, 93, 2007.

[5] Sauser R. Seppey D. Beny J.-L. Meister J.-J. Koenigsberger, M. Calcium dynamics and vosomotion in arteries subject to isometric, isobaric and isotonic conditions. *Biophysical Journal*, 95, 2008.

[6] J. Rosenberg and M. Svobodová. Comments on the thermodynamical background to the growth and remodelling theory applied to the model of muscle fibre contraction. *Applied and Computational Mechanics*, 4(1):101–112, 2010.

[7] J. Rosenberg. Modelling of the voiding process. Extended abstracts, 27th Conference with international participation Computational Mechanics, November 7.-9., Plzeň, Czech Republic, 2011.

[8] J. Rosenberg. Smooth muscle model applied to bladder. Proceeding of the 4th International conference Modelling of mechanical and mechatronic systems MMaMS, Sept. 20-22, Herlany, Slovakia, 2011.

[9] A. Dicarlo and S. Quiligotti. Growth and balance. *Mechanics Research Communications*, 29, 2002.

[10] V.N. Pokrovski. Extended thermodynamics in a discrete/system approach. *European Journal of Physics*, 26, 2005.

[11] J. Laforet and D. Guiraud. Smooth Muscle Model For Functional Electric Stimulation Applications. Proceedings of the 29th Annual International Conference of the IEEE EMBS, August 23-26, Lyon, France, 2007.

[12] Bovendeerd P.H.M. Prinzen F.W. Reneman R.S. Arts, T. Relation between left ventricular cavity pressure and volume and systolic fiber stress and strain in the wall. *Biophys. J.*, 59, 1991.

[13] Tardy Y. Meister J.-J. Stergiopulos, N. Nonlinear Separation of Forward and Backward Running Waves in Elastic Conduits. *Journal of Biomechanics*, 26, 1993.

[14] Tadmor E. Kurganov, A. New High-Resolution Central Schemes for Nonlinear Conservation Laws and Convection-Diffusion Equations. *Journal of Computational Physics*, 160(1):241–282, 2000.

[15] Vukovič S. Sopta-L. Črnjarič Zič, N. Balanced finite volume WENO and central WENO schemes for the shallow water and the open-channel flow equations. *Journal of Computational Physics*, 200(2):512–548, 2004.

[16] L. George, D. Augmented Riemann Solvers for the Shallow Water Equations over Variable Topography with Steady States and Inundation. *Journal of Computational Physics*, 227, 2008.

[17] H. Kopincová M. Brandner, J. Egermaier. Augmented Riemann solver for urethra flow modelling. *Mathematics and Computers in Simulations*, 80(6):1222–1231, 2009.

[18] R. J. Leveque. *Finite Volume Methods for Hyperbolic Problems.* Cambridge University Press, 2002.